Loop B Is a Major Structural Component of the 5-HT$_3$ Receptor

A. J. Thompson,* M. Lochner,† and S. C. R. Lummis*
*Department of Biochemistry, University of Cambridge, Cambridge, CB2 1QW, United Kingdom; and †Department of Chemistry, University of Warwick, Coventry CV4 7AL, United Kingdom

ABSTRACT The 5-HT$_3$ receptor belongs to a family of therapeutically important neurotransmitter-gated receptors whose ligand binding sites are formed by the convergence of six peptide loops (A-F). Here we have mutated 15 amino acid residues in and around loop B of the 5-HT$_3$ receptor (Ser-177 to Asn-191) to Ala or a residue with similar chemical properties. Changes in [^{3}H]granisetron binding affinity (K_d) and 5-HT EC_{50} were determined using receptors expressed in human embryonic kidney 293 cells. Substitutions at all but one residue (Thr-181) altered or eliminated binding for one or both mutants. Receptors were nonfunctional or EC_{50} values were altered for all but two mutants (S182T, I190L). Homology modeling indicates that loop B contributes two residues to a hydrophobic core that faces into the β-sandwich of the subunit, and the experimental data indicate that they are important for both the structure and the function of the receptor. The models also show that close to the apex of the loop (Ser-182 to Ile-190), loop B residues form an extensive network of hydrogen bonds, both with other loop B residues and with adjacent regions of the protein. Overall, the data suggest that loop B has a major role in maintaining the structure of the region by a series of noncovalent interactions that are easily disrupted by amino acid substitutions.

INTRODUCTION

The 5-HT$_3$ receptor is a Cys-loop receptor, which plays a role in synaptic transmission in both the central and peripheral nervous systems (1). These proteins consist of five symmetrically arranged subunits; each subunit has a large extracellular N-terminal domain that is responsible for ligand binding, four transmembrane domains (M1–M4) that surround a central ion conducting pore, and a large intracellular loop that influences channel conductance and mediates the actions of intracellular messengers. The ligand binding site is at the interface of two adjacent subunits and is formed by the convergence of three amino acid loops (A–C) from the ''principal'' subunit and three β-strands (D–F) from the ''complementary'' subunit (2).

Structural insight of this region has been gained from high resolution structures of homologous acetylcholine binding proteins (AChBPs), and nACh and bacterial receptors (2–7), and specific interactions between amino acid residues and a range of 5-HT$_3$ receptor ligands have been identified within loops A–F (8–11). Using structures of AChBP derived from crystals, and from cryo-electron microscopy data of the nACh receptor, a number of Cys-loop homology models have been published; the recent high resolution structure of a nACh receptor subunit has confirmed the accuracy of such models for the nACh receptor (6). For other receptors, however, sequence identity is only in the region of 10–20% and experimental evidence is required to support the structural accuracy of these models at the molecular level. Here we explore the roles of each residue of loop B, as the specific functions of the majority of these residues are currently unknown. The data from extensive mutagenesis, binding and functional studies reveal the importance of these residues and also provide a structural explanation for their critical roles.

EXPERIMENTAL PROCEDURES

Materials

All cell culture reagents were obtained from Gibco BRL (Paisley, UK), except fetal calf serum which was from Labtech International (Ringmer, UK). [^{3}H]granisetron (63.5 Ci/mmol) was from PerkinElmer (Boston, MA). All other reagents were of the highest obtainable grade.

Cell culture

Human embryonic kidney (HEK) 293 cells were maintained on 90 mm tissue culture plates at 37°C and 7% CO_2 in a humidified atmosphere. They were cultured in DMEM:F12 (Dulbecco's modified Eagle's medium/Nutrient Mix F12 (1:1)) with GlutaMAX I media containing 10% fetal calf serum. For radioligand binding studies cells in 90 mm dishes were transfected using calcium phosphate precipitation at 80–90% confluency and incubated for 3–4 days before use; optimization of the original method (12) by Jordon (13) resulted in increased levels of binding, which has allowed us to obtain binding parameters for mutant receptors that in the past have been expressed at levels too low to measure (e.g., W183Y and H185A). For functional studies, cells were transfected by electroporation using the AMAXA system (Amaxa GmbH, Cologne, Germany), plated on 96 well plates and incubated 1–2 days before assay.

Site-directed mutagenesis

Mutagenesis reactions were performed using the method described by Kunkel (14) using 5-HT$_{3A}$ receptor subunit cDNA (Accession: AY605711)

Submitted April 18, 2008, and accepted for publication July 30, 2008.

A. J. Thompson and M. Lochner contributed equally to this work.

Address reprint requests to Sarah C. R. Lummis, Dept. of Biochemistry, University of Cambridge, Cambridge, CB2 1QW, UK. Tel: 44-1223-765950; Fax: 44-1223-333345; E-mail: sl120@cam.ac.uk.

Editor: David S. Weiss.

0006-3495/08/12/5728/09 $2.00

doi: 10.1529/biophysj.108.135624

in pcDNA3.1 (Invitrogen, Paisley, UK) as described previously (15). A silent restriction site was incorporated into each primer to assist rapid identification.

Radioligand binding

This was undertaken as previously described with minor modifications (15). Briefly, transfected HEK293 cell membranes were incubated in 0.5 ml HEPES buffer containing the 5-HT$_3$ receptor antagonist [^{3}H]granisetron (0.1–40 nM). Nonspecific binding was determined using 1 μM quipazine. Incubations were terminated by filtration, thus limiting our determination of K_d values to $\leq$10 nM, as separation of bound from free ligand would be too slow to determine K_d values greater than this (16). Data were analyzed by iterative curve fitting (Prism v3.0, GraphPad Software, San Diego, CA) according to the equation: $B = (B_{max} \times [L])/(K + [L])$, where B is bound radioligand, B_{max} is maximum binding at equilibrium, K is the equilibrium dissociation constant, and $[L]$ is the free concentration of radioligand. Values are presented as mean $\pm$ SE. Statistical analysis was performed using ANOVA in conjunction with a Dunnett's post test.

Immunofluorescence

This was as described previously (17). Briefly, transfected cells were fixed (4 % paraformaldehyde) and incubated overnight at 4°C in pAb120 at 1:1000 in Tris-buffered saline (0.1 M Tris pH7.4, 0.9 % NaCl). Biotinylated anti-rabbit IgG (Vector Laboratories, Burlingame, CA) and fluorescein isothiocyanate avidin D (Vector Laboratories) were used to detect bound antibody as instructed by the manufacturer. Coverslips were mounted in Vectashield HardSet mounting medium (Vector Laboratories). Immuno-fluorescence was observed using an UltraVIEW LCI Confocal Imaging System (PerkinElmer).

FlexStation analysis

This technique uses fluorescent voltage-sensitive dyes to detect changes in the membrane potential and has been used to examine a range of ion channels including 5-HT$_3$ receptors (19,20). The methods were as previously described (19). Briefly, fluorescent membrane potential dye (Molecular Devices, Wokingham, UK) was diluted in Flex buffer (10 mM HEPES, 115 mM NaCl, 1 mM KCl, 1 mM $CaCl_2$, 1 mM $MgCl_2$, 10 mM glucose, pH 7.4) and added to transfected cells grown on a 96-well plate. The cells were incubated at room temperature for 45 min and then fluorescence was measured in a FlexStation (Molecular Devices) every 2 s for 200 s. Control (Flex buffer) or 5-HT (0.001 μM–1.0 mM) was added to each well after 20 s. The percent change in fluorescence was calculated as F (peak fluorescence) minus F_{min} (baseline fluorescence at 20 s) divided by F_{max} (peak fluorescence at 30 μM 5-HT). Concentration-response data were fitted to the four-parameter logistic equation, $F = F_{min} + (F_{max} - F_{min})/(1 + 10^{(\log(EC_{50} - [A]) \times nH)})$, where F_{max} is the maximum response, F_{min} is the baseline fluorescence, $[A]$ is the log concentration of agonist, and nH is the Hill coefficient, using Prism software (GraphPad). EC_{50} values determined using this technique are often slightly lower than values determined using electrophysiological studies as different phenomena are being measured: For electrophysiological studies, EC_{50} values represent the agonist concentration required to open 50% of channels, whereas in fluorescent studies they represent the agonist concentration required to depolarize the membrane potential to 50% of its original value. However, relative values for different mutant 5-HT$_3$ receptors are the same, and as cellular events are triggered by changes in membrane potential, this may be a more accurate indication of the ligand potency in vivo (19).

Modeling

This was performed as described previously (9,21). Three-dimensional models of the extracellular region of the 5-HT$_3$ receptor were built using MODELER 6v2 (22) based on the crystal structure of AChBP in different states; unbound (Protein Data Bank (PDB) ID 2byn), agonist bound (carbomylcholine, PDB ID 1uv6 and epibatidine, PDB ID 2byq) and antagonist bound (2-methyllcaconitine, PDB ID 2byr and α-cobratoxin, PDB ID 1yi5). Models were energy minimized in SYBYL v6.8 using the AMBER force field (23). Models and predicted hydrogen bonds were viewed using PyMOL v 0.98.

RESULTS

Effects of mutations

All 15 amino acids within a contiguous sequence of the 5-HT$_{3A}$ receptor subunit (Fig. 1) were mutated to either Ala or an amino acid with properties similar to the wild-type amino acid (subsequently referred to as a conserved amino acid change). Mutant receptors were characterized using [^{3}H]granisetron binding to explore changes in the ligand binding site (Table 1, Fig. 2), and 5-HT induced changes in membrane potential were measured using a voltage-sensitive fluorescent dye (Table 2, Fig. 2). Wild-type receptors had a [^{3}H]granisetron binding affinity (K_d) of 0.5 nM ($n = 11$) and 5-HT EC_{50} of 0.24 μM ($n = 12$), values that are similar to those previously published using the same techniques (15,24,25).

Alanine mutations

Amino acid substitutions to Ala revealed significant changes in [^{3}H]granisetron binding affinities for 9 of the 15 residues (Table 1). At Phe-180, Trp-183, Asp-189, Ile-190 and Asn-191, substitution with Ala eliminated any measurable binding, indicating a particularly important role for these residues. Data from the functional assay indicated a more significant effect on function as only 5 of the Ala substitutions were functional (T181A, W183A, L184A, T186A and I187A), and each of these displayed a significant increase in the EC_{50} when compared to wild-type responses.

Conserved mutations

Amino acid substitutions with conserved residues showed significant changes in [^{3}H]granisetron binding affinities for 10 of the 15 residues (Table 1). Five of these were identical to residues that had displayed sensitivity to Ala mutation (Leu-178, Phe-180, Trp-183, Asp-189, Asn-191). For the remaining five conserved mutations that displayed altered K_d values (Ser-177, Ser-182, His-185, Thr-186, Gln-188), there was no corresponding change in affinity for the Ala mutants, indicating that it was not the chemical characteristics of the residue that was critical at these positions. Mutations at Leu-178, Gln-188 and Asp-189 caused complete ablation of [^{3}H]granisetron binding. In the functional assay five conserved mutations were functional (S182T, W183Y, L184I, I187L, I190L). Three of these displayed smaller increases in EC_{50} than their Ala counterparts (W183Y, L184I, I187L), whereas S182T and I190L had values that were not significantly different to wild-type receptors.

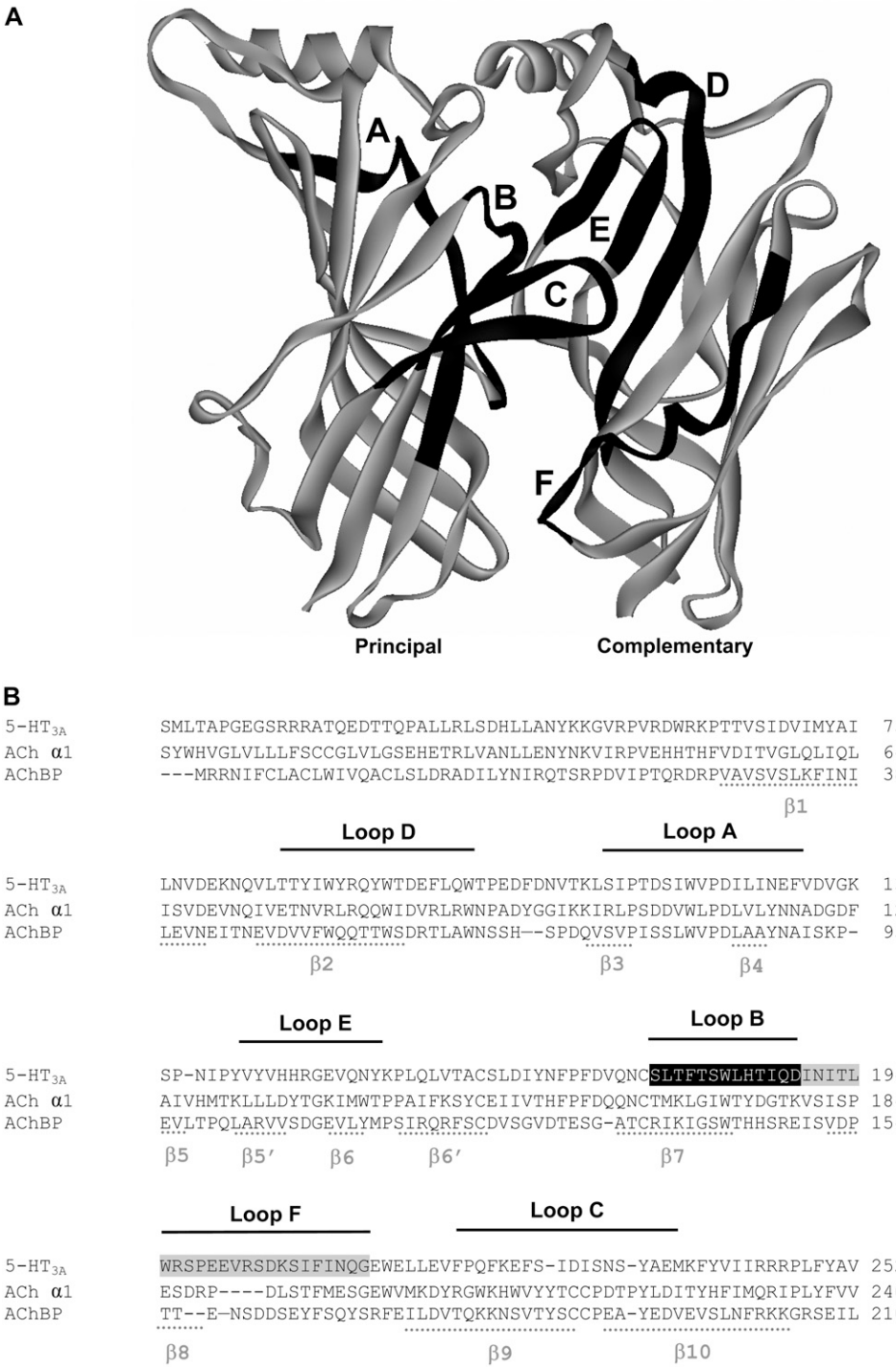

FIGURE 1 Location of the amino acid residues examined in the current study. (*A*) Two adjacent subunits (*principal* and *complementary*), showing the positions of the six binding loops A-F. (*B*) The amino acid sequence for the extracellular domain of the murine 5-HT_{3A} receptor (accession No. Q6J1J7), aligned with AChBP isolated from *Lymnaea stagnalis* (P58154) and the nACh receptor α1 subunit (P02710). The residues examined are highlighted as white text on a black background. Loop F residues that we have reported on previously are highlighted as white text on a gray background (25). The six binding loops are indicated by black lines above the text. The positions of β-sheets are shown by gray lines beneath the text. Numbering of residues and structural features are taken from the AChBP protein crystal structure (3).

Immunocytochemistry

For mutants that were classified as having no specific radioligand binding, cell surface expression was studied using immunofluorescence and confocal microscopy. Fig. 3 shows that of the eight mutants, four were not expressed at the cell surface (F180A, Q188N, D189A and I190A). The remaining mutants (L178I, W183A, D189E and N191A) all showed a distinct halo of fluorescence at the cell surface, indicating that the receptors were correctly assembled and trafficked to the plasma membrane.

Loop B modeling

To gain further insight into the possible orientations and interactions of loop B residues, a range of homology models were constructed based on AChBP crystal structures that

TABLE 1 Effects of Ala and conserved substitutions on [^{3}H]granisetron binding affinities at the 5-HT$_3$ receptor

Alanine mutant	pK$_d$ (nM) Mean ± SE	K_d (nM)	n	Conserved mutant	pK$_d$ (nM) Mean ± SE	K_d (nM)	n
Wild-type	9.30 ± 0.12	0.5	11	Wild-type	9.30 ± 0.12	0.5	11
S177A	9.23 ± 0.26	0.7	5	S177T	7.86 ± 0.09†	14*	3
L178A	8.02 ± 0.09†	10	4	L178I	NB†	—	4
T179A	8.55 ± 0.09†	3.2	8	T179S	9.33 ± 0.22	0.5	7
F180A	NB†	—	5	F180Y	8.19 ± 0.08†	6.5	3
T181A	9.38 ± 0.18	0.4	7	T181S	9.15 ± 0.11	0.7	4
S182A	9.06 ± 0.10	0.9	6	S182T	8.71 ± 0.03†	1.9	8
W183A	NB†	—	6	W183Y	8.38 ± 0.10†	4.2	6
L184A	8.42 ± 0.10†	4.1	4	L184I	9.12 ± 0.03	0.8	6
H185A	8.86 ± 0.11	1.4	5	H185N	8.45 ± 0.07†	3.5	5
T186A	9.26 ± 0.06	0.6	9	T186S	8.17 ± 0.06†	6.8	4
I187A	7.90 ± 0.04†	13*	4	I187L	8.90 ± 0.14	1.3	8
Q188A	9.22 ± 0.15	0.6	7	Q188N	NB†	—	4
D189A	NB†	—	4	D189E	NB†	—	7
I190A	NB†	—	5	I190L	8.93 ± 0.02	1.2	4
N191A	NB†	—	5	N191Q	8.20 ± 0.11†	6.3	4

†Significantly different when compared to wild-type (ANOVA with Dunnett's post test: $p < 0.05$). NB, No binding or K_d values ≥ 10 nM, which is the resolution of the technique (16); thus values obtained that are >10 nM (*) may be inaccurate.

TABLE 2 Functional effects of Ala and conserved substitutions at the 5-HT$_3$ receptor

Alanine mutant	pEC_{50} Mean ± SE	EC_{50} (μM)	n	Conserved mutant	pEC_{50} Mean ± SE	EC_{50} (μM)	n
Wild-type	6.62 ± 0.06	0.24	12	Wild-type	6.62 ± 0.06	0.24	12
S177A	NR*	—	4	S177T	NR*	—	4
L178A	NR*	—	4	L178I	NR*	—	4
T179A	NR*	—	4	T179S	NR*	—	4
F180A	NR*	—	4	F180Y	NR*	—	4
T181A	5.86 ± 0.08*	1.38	4	T181S	NR*	—	6
S182A	NR*	—	4	S182T	6.21 ± 0.07	0.62	4
W183A	4.40 ± 0.11*	39.8	6	W183Y	5.28 ± 0.26*	5.25	6
L184A	4.47 ± 0.07*	33.9	4	L184I	5.47 ± 0.17*	3.39	4
H185A	NR*		4	H185N	NR*	—	4
T186A	4.24 ± 0.03*	57.5	6	T186S	NR*	—	4
I187A	4.65 ± 0.07*	22.4	4	I187L	5.48 ± 0.10*	3.31	4
Q188A	NR*		4	Q188N	NR*	—	4
D189A	NR*		4	D189E	NR*	—	4
I190A	NR*		4	I190L	6.33 ± 0.01	0.47	4
N191A	NR*		4	N191Q	NR*	—	4

*Significantly different to wild-type (ANOVA with Dunnett's post test: $p <$ 0.05). NR, No response.

were either unbound or bound by different ligands. The lowest energy states for the models are shown in Fig. 4, *A–E*, and the carbon backbones for each of these are overlaid in Fig. 4 *F*. Loop B is similar in each of these models, suggesting that regardless of the bound ligand, the position of the loop and the orientations of the side-chains remains relatively unaltered.

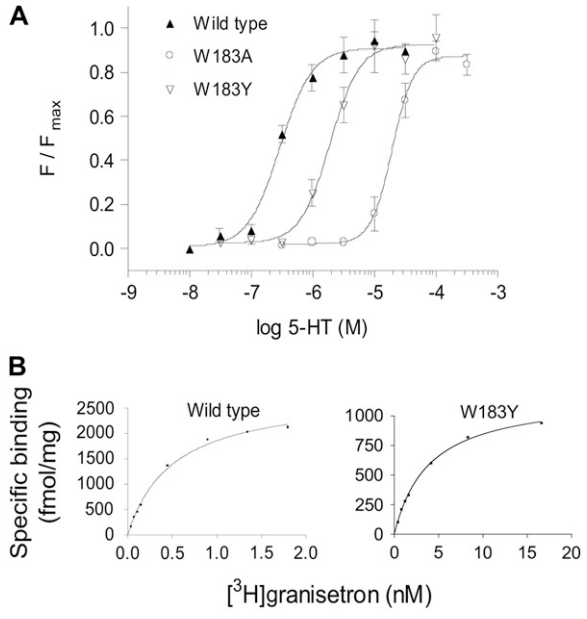

FIGURE 2 Example data for receptor function and radioligand binding at wild-type and mutant receptors. (*A*) Channel function was measured using a voltage-sensitive fluorometric dye on a FlexStation. Values from a series of experiments were normalized, averaged and fitted with a four-parameter logistic equation. The calculated EC_{50} values are shown in Table 2. (*B*) K_d values were estimated using the 5-HT$_3$ antagonist [^{3}H]granisetron. The examples show binding for single experiments, fitted with a one site binding equation. K_d values for a series of experiments were averaged for each mutant, and are presented in Table 1.

The models indicate that there is a hydrophobic core between the inner and outer β sheets (Fig. 5, *A* and *B*). They also predict an extensive network of hydrogen bonds, both between loop B and adjacent regions, and within the B loop itself (Fig. 5, *C* and *D*). In the first group, the β-strand of loop B is stabilized by hydrogen bonds between the backbones of residues from Leu-178 to His-185, and the adjacent anti-parallel strands of β4 and β10, and the backbones of Asp-189 and Asn-191 form hydrogen bonds with the backbones of Thr-64 and Val-66 in the adjacent β1-strand. The second group includes the side-chains of residues His-185, Gln-188 and Asp-189 which stabilize a tight β7-β8 turn at the top of loop B. Our homology models predict that amino acid substitutions in this region would disrupt this hydrogen bonding network (Fig. 5, *E–H*).

DISCUSSION

This study shows that the 5-HT$_3$ receptor loop B is extremely sensitive to amino acid changes; our data show that substitutions of most of the residues from Ser-177 to Asn-191 have a significant effect on [^{3}H]granisetron binding and 5-HT evoked currents. Loop B in all Cys-loop receptors has long been known to play an important role in receptor function, but it was surprising that so many of the residues in this region were sensitive to amino acid substitution. A possible explanation for these data is provided by our homology models, which show that many of these residues could stabilize the structure of the region through hydrophobic interactions and hydrogen bonds.

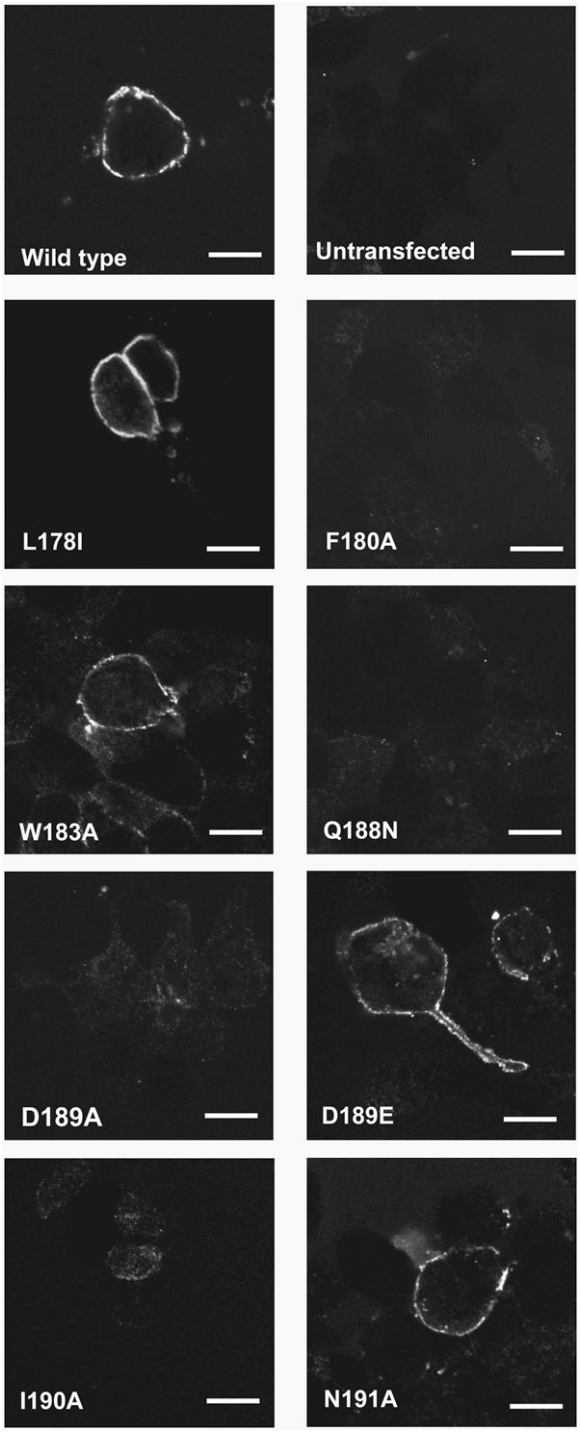

FIGURE 3 Cell surface expression of mutant 5-HT_3 receptors. Typical images of wild-type and mutant receptors revealed by immunofluorescent labeling of nonpermeabilized transfected HEK 293 cells using a 5-HT_3-specific antisera (18). Scale bar, 25 μm.

Loop B is a stable, static structure

Comparing a range of homology models based on AChBP bound to different agonists (which are presumed to represent the open state of the receptor), and antagonists (the closed state), shows that loop B is similarly positioned in each of the models. This indicates that there is little or no movement of this loop between the open and closed states, suggesting a stable and static structure that does not change conformation when ligands bind. Our homology models indicate that loop B residues could play an important role in stabilizing the structure of the whole region, as many loop B residues contribute to a global network of noncovalent interactions. In agreement, a similar homology-based study has found that distances between Trp-183 residues of adjacent 5-HT_3 subunits were comparable regardless of the AChBP template used (25). Data from previous studies also indicate that this region of the protein has an important structural role in homologous receptors. For example, in the nACh receptor the loop B residue Lys-145 (equivalent to Thr-179 in the 5-HT_3 receptor) has been shown to form a salt-bridge with Asp-200 (Glu-236 in 5-HT_3), and is proposed as one of a number of strong interactions that stabilize the binding region in this receptor (26). We must, of course, be cautious when using bound AChBP structures as templates for open and closed states of the receptor, but comparisons with nACh receptor structures and molecular dynamic simulations indicate they are reasonably accurate (3,5,6,27). This observation is further supported by the more recent structure determination of a homologous prokaryotic ion channel (7).

Loop B contributes to a hydrophobic core

Our modeling data indicate that in each subunit there is a central hydrophobic core formed by the converging side chains of residues distributed throughout the 5-HT_3 receptor subunit sequence. The residues are mostly located in the inner and outer β-sheets comprising the β-sandwich of the extracellular part of the subunit, and their side chains all point into the interior of the β-sandwich (see Figs. 1 and 5). Two of these residues are contributed by loop B, and these are surrounded by other hydrophobic residues; Leu-178 is surrounded by Ile-127, Phe-130, Phe-180 and Phe-239, whereas Phe-180 is surrounded by Val-70, Tyr-91, Ile-125, Ile-127, Leu-178 and Phe-239. In total there are 16 hydrophobic residues within 5 Å of Leu-178 and Phe-180 (Fig. 5). This region may be critical for receptor folding, as hydrophobic regions are usually the first to form, and indeed our data suggest that substituting Phe-180 for Ala prevents correct assembly and targeting of the receptor. Tyr-91 and Phe-130 have also been proposed to play a role in assembly and/or targeting (15,28). We suggest, therefore, that this hydrophobic region is important for the correct folding and assembly of the 5-HT_3 receptor, and as 15 of the 16 hydrophobic residues align with hydrophobic residues across the entire Cys-loop family, this region probably has a similar role in all Cys-loop receptors.

Our data also suggest that this region has a role in receptor function. The mutations L178A and F180Y both yield receptors that bind antagonist, indicating that these receptors are correctly assembled and targeted, and their binding sites

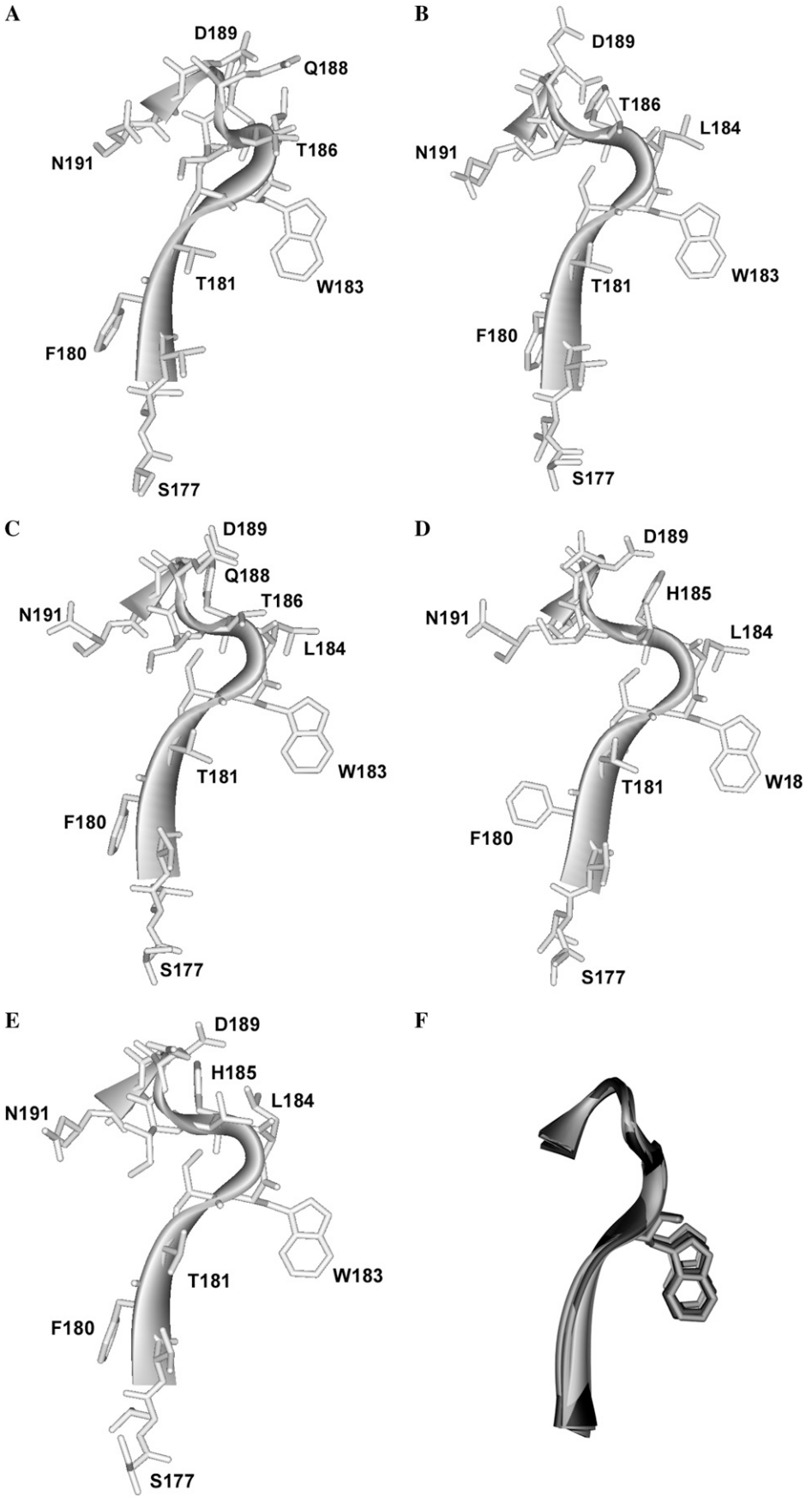

FIGURE 4 Homology models showing the amino acid backbone of the loop B region of the 5-HT$_3$ receptor. (*A*) Unbound structure (modeled from AChBP with no ligand, PDB ID 2byn). (*B*) Agonist bound, (modeled from AChBP with carbomylcholine, PDB ID 1uv6). (*C*) Agonist bound, (modeled from AChBP with epibatidine, PDB ID 2byq). (*D*) Large antagonist bound (modeled from AChBP with α-cobratoxin, PDB ID 1yi5). (*E*) Small antagonist bound, (modeled from AChBP with 2-methyllcaconitine, PDB ID 2byr) (*F*) Overlays of the modeled loop B backbones from *A–E* compiled with Swiss-PdbViewer ''magic fit'', using residues Ser-177 to Asn-191 as a reference point.

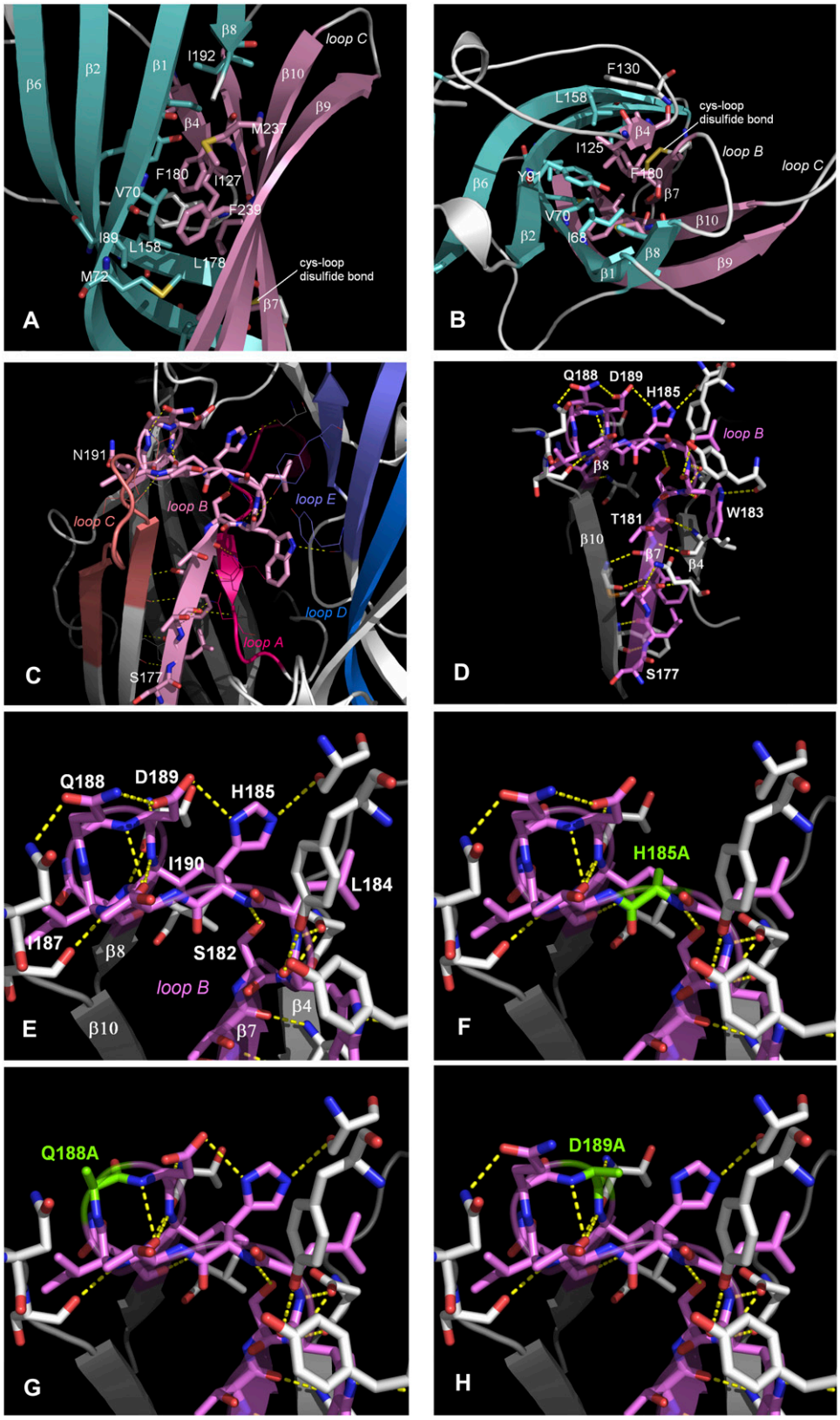

FIGURE 5 Models of the loop B region of the 5-HT_3 receptor. Side (*A*) and top (*B*) views of the hydrophobic core of the β-sandwich around Leu-178 and Phe-180. Loop F and a short stretch between the N-terminus and β1 have been omitted for clarity. Inner β-sheets in aquamarine, outer β-sheets in pink. Hydrophobic residues within 5 Å of Leu-178 and Phe-180 are rendered in stick representation and color coded according to the corresponding β-sheets. This hydrophobic core includes Ile-68, Val-70, Met-72, Leu-85, Ile-89, Tyr-91, Ile-125, Ile-127, Phe-130, Leu-158, Leu-178, Phe-180, Ile-192, Met-237, Phe-239, and Val-241. The hydrophobic nature of these residues is conserved across the Cys-loop family (see Fig 1). (*C*) The distribution of potential hydrogen bonds between loop B and adjacent regions. (*D*) Hydrogen bonds between residues within loop B. Hydrogen bonds that may stabilize the β7-β8 turn are shown in *E*, and mutation of these residues (*F–H*) could disrupt this pattern. Hydrogen bonds in this figure were predicted, and are visualized, using PyMOL v 0.98.

are intact. However they do not function. We propose that specific hydrophobic interactions in this part of loop B are a critical component of a hydrophobic core, where weak and easily interchangeable interactions are necessary for the lateral movement of the outer and inner β-sheets when a ligand binds (a proposed step in the transduction pathway that ultimately leads to pore opening (29)).

Loop B contributes to receptor gating

In addition to the gating role played by residues in the hydrophobic core, we propose that other amino acids in loop B also have a significant role in channel function. One of these residues is Leu-184 which displays an ~10-fold increase in EC_{50} with a conservative Ile substitution, but shows very little change in antagonist binding affinity, as previously reported (9). EC_{50} is constituted from both agonist affinity and functional efficacy. The agonist affinity can be modified by mutations that cause a structural change in the binding site, or when an agonist-specific binding residue is altered. The antagonist binding data show there is no structural change in the binding site with L184I mutant receptors, and the modeling data face Leu-184 away from the binding pocket; thus it is unlikely to be an agonist-specific ligand binding residue. The data therefore support a role for this residue in the conformational changes that follow, or are concomitant with, ligand binding, and that ultimately result in channel opening. In support of this hypothesis the adjacent residue Trp-183, which has been shown to be involved in agonist binding (30–33), is located facing into the binding pocket in the model, and the mutation W183Y results in a similar fold change in antagonist affinity and EC_{50}, suggesting it is primarily the affinity change that causes the change in EC_{50}.

Our models suggest a mechanism by which Leu-184 could be involved in channel opening: via hydrogen bonds with the adjacent β-sheet of loop A. There is evidence that loop A plays a dynamic role during receptor gating and it has been proposed that it acts as a ''latch' that controls this process in the nACh receptor (20). In addition, reorientations in this region have been shown with molecular dynamic studies (27). Our data suggest that a small residue at position 184 is much less favorable than a larger one, and we propose that to allow movement, Leu-184 may function as a 'spacer' residue, holding loop B at an optimal distance from loop A and thereby allowing movement of the latter. Similarly, 'spacer' residues may be important to allow movement of loop C, as a bulky hydrophobic side chain was preferred at position 187 (loop B), and our homology models suggest van der Waals contacts between the side chain of Ile-187 and residues within the β9 and β10 strands (loop C) of the same subunit. Thus Ile-187 may sterically oppose the β9 and β10 strands and thereby assure the mobility of loop C. We propose that loop B forms a rigid frame around which loops A and C move.

Other residues that may play a role in channel function are Thr-179, Thr-181, Ser-182, His-185 and Thr-186 as mutation of all of these significantly affected agonist-mediated effects, but neither Ala nor conserved mutations caused major changes in the antagonist binding affinity; the latter results indicating the receptors are correctly assembled. However, loss of the backbone hydrogen bonding between these residues and the adjacent β-sheets, as indicated in the homology models, may prevent efficient opening of the channel. It should also be noted that in previous studies H185A has been reported as nonbinding, a difference that is likely to reflect the very low levels of expression (~20-fold less than wild-type) that we observed for this mutant (11). Binding affinities for Thr-179, Ser-182 and Thr-186 mutants are almost identical to those shown elsewhere (9).

Our homology models also suggest that there are hydrogen bonds contributed by residues His-185 to Asn-191 which may be important for stabilizing the β7 - β8 turn; substitution of residues that significantly disrupt this series of bonds (Q188, D189 and I190; Fig. 5, *G* and *H*) results in receptors that are not folded, assembled and/or targeted correctly. Substitutions that permit the expression of cell-surface receptors, possibly because they disrupt fewer hydrogen bonds (such as in H185A), may result in low levels of expression or non functional receptors. We propose that a rigid β7-β8 turn is critical for efficient receptor expression and function. Asp-189 may also have a role in subunit-subunit interactions, similar to the equivalent residue (Glu-149) in AChBP (3,11). In our 5-HT$_3$ homology models Asp-189 is in close proximity to the basic side chains of Lys-112 on the complementary subunit and a highly conserved Arg-55 on the same subunit, and there is the potential to form a salt bridge here, an interaction that would explain why substitution of this residue was especially sensitive; it was the only residue where both Ala and conserved amino acid substitutions yielded non binding receptors.

CONCLUSIONS

We have demonstrated that residues from the 5-HT$_3$ receptor loop B region have a major influence on binding and function. These data can be explained by our model, which indicates that noncovalent interactions within and between loop B and neighboring residues, both in the binding region and within the β-sandwich structure of the subunit, are vital for the integrity of the binding site and for the dynamic mobility of structural elements involved in the gating process.

We thank the Wellcome Trust for funding (S.C.R.L. and A.J.T.) and the Swiss National Science Foundation for a postdoctoral fellowship to M.L. (PA00A-105073). S.C.R.L. is a Wellcome Trust Senior Research Fellow in Basic Biomedical Studies.

REFERENCES

1. Thompson, A. J., and S. C. R. Lummis. 2007. The 5-HT$_3$ Receptor as a therapeutic target. *Expert Opin. Ther. Targets*. 11:527–540.

2. Brejc, K., W. J. van Dijk, R. V. Klaassen, M. Schuurmans, J. van Der Oost, A. B. Smit, and T. K. Sixma. 2001. Crystal structure of an ACh-binding protein reveals the ligand-binding domain of nicotinic receptors. *Nature*. 411:269–276.
3. Celie, P. H., S. E. van Rossum-Fikkert, W. J. van Dijk, K. Brejc, A. B. Smit, and T. K. Sixma. 2004. Nicotine and carbamylcholine binding to nicotinic acetylcholine receptors as studied in AChBP crystal structures. *Neuron*. 41:907–914.
4. Celie, P. H., R. V. Klaassen, S. E. van Rossum-Fikkert, R. van Elk, P. van Nierop, A. B. Smit, and T. K. Sixma. 2005. Crystal structure of acetylcholine-binding protein from *Bulinus truncatus* reveals the conserved structural scaffold and sites of variation in nicotinic acetylcholine receptors. *J. Biol. Chem.* 280:26457–26466.
5. Unwin, N. 2005. Refined structure of the nicotinic acetylcholine receptor at 4Å resolution. *J. Mol. Biol.* 346:967–989.
6. Dellisanti, C. D., Y. Yao, J. C. Stroud, Z. Z. Wang, and L. Chen. 2007. Crystal structure of the extracellular domain of nAChR α1 bound to α-bungarotoxin at 1.94 Å resolution. *Nat. Neurosci.* 10:953–962.
7. Hilf, R. J., and R. Dutzler. 2008. X-ray structure of a prokaryotic pentameric ligand-gated ion channel. *Nature*. 452:375–379.
8. Thompson, A. J., and S. C. Lummis. 2006. 5-HT_3 receptors. *Curr. Pharm. Des.* 12:3615–3630.
9. Thompson, A. J., K. L. Price, D. C. Reeves, S. L. Chan, P. L. Chau, and S. C. Lummis. 2005. Locating an antagonist in the 5-HT_3 receptor binding site using modeling and radioligand binding. *J. Biol. Chem.* 280:20476–20482.
10. Yan, D., and M. M. White. 2005. Spatial orientation of the antagonist granisetron in the ligand-binding site of the 5-HT_3 receptor. *Mol. Pharmacol.* 68:365–371.
11. Joshi, P. R., A. Suryanarayanan, E. Hazai, M. K. Schulte, G. Maksay, and Z. Bikadi. 2006. Interactions of granisetron with an agonist-free 5-HT_{3A} receptor model. *Biochemistry.* 45:1099–1105.
12. Chen, C. A., and H. Okayama. 1988. Calcium phosphate-mediated gene transfer: a highly efficient transfection system for stably transforming cells with plasmid DNA. *Biotechniques.* 6:632–638.
13. Jordan, M., A. Schallhorn, and F. M. Wurm. 1996. Transfecting mammalian cells: optimization of critical parameters affecting calcium-phosphate precipitate formation. *Nucleic Acids Res.* 24:596–601.
14. Kunkel, T. A. 1985. Rapid and efficient site-specific mutagenesis without phenotypic selection. *Proc. Natl. Acad. Sci. USA*. 82:488–492.
15. Price, K. L., and S. C. Lummis. 2004. The role of tyrosine residues in the extracellular domain of the 5-hydroxytryptamine$_3$ receptor. *J. Biol. Chem.* 279:23294–23301.
16. Bylund, D. B., and M. L. Toews. 1993. Radioligand binding methods: practical guide and tips. *Am. J. Physiol.* 265:421–429.
17. Spier, A. D., G. Wotherspoon, S. V. Nayak, R. A. Nichols, J. V. Priestley, and S. C. R. Lummis. 1999. Antibodies against the extracellular domain of the 5-HT_3 receptor label both native and recombinant receptors. *Brain Res. Mol. Brain Res.* 67:221–230.
18. Fitch, R.W., Y. Xiao, Y., K.J. Kellar, and J. W. Daly. 2003 Membrane potential fluorescence: a rapid and highly sensitive assay for nicotinic receptor channel function. *Proc. Natl. Acad. Sci. USA*. 100:4909–4914.
19. Price, K. L., and S. C. Lummis. 2005. FlexStation examination of 5-HT(3) receptor function using Ca^{2+}- and membrane potential-sensitive dyes: advantages and potential problems. *J. Neurosci. Methods*. 149: 172–177.
20. Chakrapani, S., T. D. Bailey, and A. Auerbach. 2003. The role of loop 5 in acetylcholine receptor channel gating. *J. Gen. Physiol.* 122:521–539.
21. Reeves, D. C., M. F. Sayed, P. L. Chau, K. L. Price, and S. C. Lummis. 2003. Prediction of 5-HT_3 receptor agonist-binding residues using homology modeling. *Biophys. J.* 84:2338–2344.
22. Sali, A., and T. L. Blundell. 1993. Comparative protein modelling by satisfaction of spatial restraints. *J. Mol. Biol.* 234:779–815.
23. Weiner, S. J., P. A. Kollman, D. A. Case, U. C. Singh, C. Ghio, G. Alagona, S. Profeta, and P. Weiner. 1984. A new force-field for molecular mechanical simulation of nucleic-acids and proteins. *J. Am. Chem. Soc.* 106:765–784.
24. Spier, A. D., and S. C. Lummis. 2000. The role of tryptophan residues in the 5-Hydroxytryptamine$_3$ receptor ligand binding domain. *J. Biol. Chem.* 275:5620–5625.
25. Thompson, A. J., C. L. Padgett, and S. C. Lummis. 2006. Mutagenesis and molecular modeling reveal the importance of the 5-HT_3 receptor F-loop. *J. Biol. Chem.* 281:16576–16582.
26. Mukhtasimova, N., C. Free, and S. M. Sine. 2005. Initial coupling of binding to gating mediated by conserved residues in the muscle nicotinic receptor. *J. Gen. Physiol.* 126:23–39.
27. Cashin, A. L., E. J. Petersson, H. A. Lester, and D. A. Dougherty. 2005. Using physical chemistry to differentiate nicotinic from cholinergic agonists at the nicotinic acetylcholine receptor. *J. Am. Chem. Soc.* 127:350–356.
28. Sullivan, N. L., A. J. Thompson, K. Price, and S. C. R. Lummis. 2006. Defining the roles of Asn-128, Glu-129 and Phe-130 in loop A of the 5-HT_3 receptor. *Mol. Membr. Biol.* 23:1–10.
29. Unwin, N., A. Miyazawa, J. Li, and Y. Fujiyoshi. 2002. Activation of the nicotinic acetylcholine receptor involves a switch in conformation of the alpha subunits. *J. Mol. Biol.* 319:1165–1176.
30. Beene, D. L., G. S. Brandt, W. Zhong, N. M. Zacharias, H. A. Lester, and D. A. Dougherty. 2002. Cation-π interactions in ligand recognition by serotonergic (5-HT_{3A}) and nicotinic acetylcholine receptors: the anomalous binding properties of nicotine. *Biochemistry.* 41:10262–10269.
31. Lummis, S. C., D. L. Beene, N. J. Harrison, H. A. Lester, and D. A. Dougherty. 2005. A cation-π binding interaction with a tyrosine in the binding site of the $GABA_C$ receptor. *Chem. Biol.* 12:993–997.
32. Zhong, W. G., J. P. Gallivan, Y. O. Zhang, L. T. Li, H. A. Lester, and D. A. Dougherty. 1998. From ab initio quantum mechanics to molecular neurobiology: A cation-π binding site in the nicotinic receptor. *Proc. Natl. Acad. Sci. USA*. 95:12088–12093.
33. Padgett, C. L., A. P. Hanek, H. A. Lester, D. A. Dougherty, and S. C. Lummis. 2007. Unnatural amino acid mutagenesis of the $GABA_A$ receptor binding site residues reveals a novel cation-π interaction between GABA and β2 Tyr97. *J. Neurosci.* 27:886–892.